Tomography of quark gluon plasma at energies available at the BNL Relativistic Heavy Ion Collider (RHIC) and the CERN Large Hadron Collider (LHC)

P. B. Gossiaux, R. Bierkandt, and J. Aichelin
SUBATECH, Université de Nantes, EMN, IN2P3/CNRS, 4 rue Alfred Kastler, F-44307 Nantes Cedex 3, France
(Received 25 July 2008; published 15 April 2009)

Using the recently published model [Gossiaux and Aichelin, Phys. Rev. C **78**, 014904 (2008)] for the collisional energy loss of heavy quarks in a quark gluon plasma (QGP), based on perturbative QCD (pQCD) with a running coupling constant, we study the interaction between heavy quarks and plasma particles in detail. We discuss correlations between the simultaneously produced c and $\bar{c}$ quarks, study how central collisions can be experimentally selected, predict observable correlations, and extend our model to the energy domain of the Large Hadron Collider (LHC). We finally compare the predictions of our model with that of other approaches such as anti-de Sitter/conformal field theory (AdS/CFT).

DOI: 10.1103/PhysRevC.79.044906 PACS number(s): 12.38.Mh, 25.75.−q

I. INTRODUCTION

High transverse momentum (p_T) single nonphotonic electrons that have been measured in the BNL Relativistic Heavy Ion Collider (RHIC) heavy-ion experiments [1,2] come dominantly from heavy-meson decay. The weighted ratio of their p_T spectra in pp and AA collisions, $R_{AA} = d\sigma_{AA}/(N_c dp_T^2)/(d\sigma_{pp}/dp_T^2)$, where N_c is the number of initial binary collisions, reveals the energy loss of heavy quarks in the environment created by AA collisions. Initially, the azimuthal distribution $d\sigma/d\phi \propto [1 + 2v_1\cos(\phi) + 2v_2\cos(2\phi)]$ of light quarks and gluons is isotropic and the anisotropy develops during the expansion as an image of the initial eccentricity in coordinate space. The heavy quarks—created in a hard process—are initially isotropically distributed in the transverse momentum space. The final v_2 of heavy quarks shows therefore how the anisotropy of the light quarks and gluons is transferred to heavy quarks and hence reflects this interaction at later times.

Recently, we have published an approach [3] in which we have shown that the energy loss as well as the $v_2(p_T)$ distribution of the single nonphotonic electrons in heavy-ion reactions can be understood in a perturbative QCD (pQCD) based model in which the heavy quarks interact with the expanding quark gluon plasma (QGP). In contradistinction to former approaches this model has two improvements: (1) a running coupling constant and (2) an infrared regulator in the t channel, which has been determined by physical requirements.

It is the purpose of this article to explore the details of the interaction between the heavy quarks and the QGP in this model, to determine the consequences for observables, to explore whether there is a simple way to describe the energy loss in this complicated environment, and to predict correlations between the simultaneously produced c and $\bar{c}$ quarks. Furthermore, we extend the model to the future CERN Large Hadron Collider (LHC) energies and confront the results with other theories such as the anti-de Sitter/conformal field theory (AdS/CFT) approach.

II. THE MODEL

The model [3] to describe the momentum distribution of heavy quarks or heavy mesons produced in ultrarelativistic heavy-ion collisions has five major parts: (1) the initial distributions of the heavy quarks, (2) the description of the expanding QGP, (3) the elementary interaction between the heavy quarks and light quarks or gluons, (4) the interaction of the heavy quarks with the plasma, and 5. the hadronization of heavy quarks into open charm and open beauty mesons. These will be described in turn.

A. Initial distribution of the heavy quarks

For the momentum-space distribution as well as for the relative contribution of charm and bottom quarks in pp collisions we use the pQCD results in fixed order plus next to leading logarithm (FONLL) of Cacciari and co-workers [4].

For RHIC energies these results have been published in Ref. [5], where a ratio of $\sigma_{\bar{b}b}/\sigma_{\bar{c}c} = 7 \times 10^{-3}$ is predicted. Nevertheless, above $p_T > p_{T\,\mathrm{cross}} \approx 4$ GeV more electrons are produced by B-meson decay than by D-meson decay. The uncertainty of $p_{T\,\mathrm{cross}}$ is, however, considerable. This is due to the uncertainty of the quark masses and of the factorization and renormalization scales, μ_F and μ_R. In this work we have taken $m_c = 1.5$ GeV and $m_b = 5.1$ GeV and have retained the values of μ_R and μ_F that correspond to the top curves in the uncertainty bands [5] and that are shown in Fig. 1. They provide, after fragmentation into D and B mesons and subsequent semileptonic decay, the closest agreement with RHIC nonphotonic single-electron data. For LHC energies the initial spectra is stiffer [6] as shown in Fig. 1. The heavy quarks are isotropically distributed in azimuthal direction and therefore their v_2 is initially zero. Any observed anisotropy of heavy mesons is due to the interaction of their constituents with the medium and can therefore be used to reveal the strength of this interaction.

In the E866 experiment at Fermi Lab [7] it has been observed that in pA collisions J/ψ mesons have a larger average transverse momentum as compared to pp collisions. This effect, called the Cronin effect, can be parametrized as an increase of $\langle p_T^2 \rangle$ by $\delta_0 \approx 0.2$ GeV^2 per collision of the incident nucleon with one of the target nucleons. We have the option of including this effect by convoluting the initial transverse-momentum distribution of the heavy quark [5]

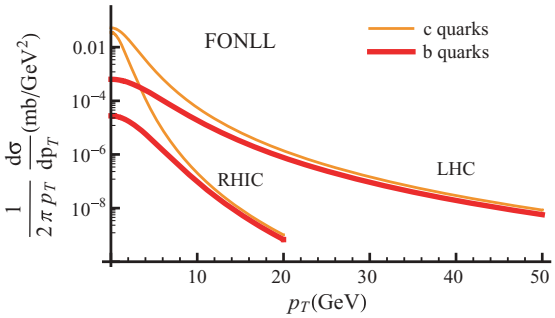

FIG. 1. (Color online) Transverse momentum distribution of c and b quarks in fixed order + next to leading logarithm (FONLL) for RHIC [5] and LHC [6].

with a Gaussian distribution of r.m.s. $\sqrt{n_{\rm coll}(\vec{r}_\perp)\,\delta_0}$. In this parametrization $n_{\rm coll}$ is taken as the mean number of soft collisions that the incoming nucleons have suffered prior to the formation of the $Q\bar{Q}$ pair at transverse position $\vec{r}_\perp$. It turned out that the Cronin effect influences the p_T spectra below $p_T \approx 5$ GeV but is without importance for higher p_T.

In coordinate space the initial distribution of the heavy quarks is given by a Glauber calculation.

B. The expanding plasma

The expanding plasma is described by a hydrodynamical approach neglecting an eventually existing hard component created by jets. We use the boost-invariant model of Heinz and Kolb, which has been described in detail in Ref. [8]. This model reproduces a variety of experimental findings. Corresponding to two different equations of state this approach allows to calculate two distinct scenarios of the expansion. Either the transition from the QGP to the hadron phase is sudden or the system traverses a mixed phase. Hadronization after the mixed phase reproduces the spectra of light mesons and is therefore favored by experimental data. Without a mixed phase also for heavy quarks the interaction time is too short [3] to reproduce the energy loss and the azimuthal anisotropy seen in the experimental RHIC data.

Therefore, we use here the model in the mixed-phase scenario. We parametrize the temperature $T(r, t)$ and the mean velocity $u(r, t)$ of this calculation. These quantities serve then to calculate the interaction of the heavy quarks with the medium. They allow us to calculate the number density of the plasma particles (and hence of the collision rate) as well as their momentum distribution.

At RHIC the initial entropy density for the hydrodynamical calculations is chosen in such a way that the experimental multiplicity $dN_{\rm ch}/dy(y = 0)$ is reproduced [8]. For the LHC prediction we assume that the soft (thermalized) component contains $1600 < dN_{\rm ch}/dy(y = 0) < 2200$.[1]

[1]This corresponds, according to the hydrodynamical calculation, to a plasma lifetime of $6.6 < \tau_{\rm QGP} < 7.4$ fm/c and to an additional lifetime of the mixed phase of ≈ 4 fm/c.

C. Elementary interaction between the heavy quarks and the plasma particles

Using a fixed coupling constant and the Debye mass ($m_D \approx g_S T$) as infrared regulator, pQCD calculations are unable to reproduce the data, neither the energy loss nor the azimuthal distribution characterized by (v_2). The novelty of the approach of Ref. [3] is a new description of the interaction between the heavy quarks and the plasma. As compared to former pQCD calculations we have introduced (a) an effective running coupling constant, $\alpha_{\rm eff}(Q^2)$, determined from electron-positron annihilation and nonleptonic decay of τ leptons and (b) an infrared regulator in the t channel, which is adjusted to give the same energy loss as calculated in a hard thermal loop approach. In standard pQCD calculations [9,10] the gluon propagator in the t-channel Born matrix element has to be IR regulated by a screening mass μ,

$$\frac{\alpha}{t} \to \frac{\alpha}{t-\mu^2}. \tag{1}$$

Frequently, the IR regulator is taken as proportional to the square of the Debye mass, m_D, [11]

$$\mu^2 = m_D^2 = \frac{N_c}{3}\left(1+\frac{1}{6}n_f\right)4\pi\alpha_S T^2 \approx (g_S T)^2, \tag{2}$$

where $n_f(N_c)$ are the number of flavors (colors), $g_S^2 = 4\pi\alpha_S$, and T is the temperature. Other approaches use the square of the thermal gluon mass, $\frac{m_D^2}{3}$ [12]. In short, μ^2 is not well determined. Braaten and Thoma [13] have shown for QED that in a medium with finite temperature the Born approximation is not appropriate for low momentum transfer $|t|$ but has to be replaced by a hard thermal loop calculation. Extending their work to QCD we have shown [3] that the energy loss, calculated with pQCD matrix elements of the form of Eq. (1), only agrees with that calculated in a hard thermal loop approach if μ^2 is much smaller and around

$$\mu^2 \approx 0.2 g_S^2 T^2. \tag{3}$$

Employing a running coupling constant and replacing the Debye mass by an effective IR cutoff [Eq. (3)] we find a substantial increase of the collisional energy loss, which brings for the RHIC experiments $v_2(p_T)$ as well as $R_{AA}(p_T)$ to values close to the experimental ones without excluding a contribution from radiative energy loss. More precisely, the collisional cross section has to be multiplied by a K factor of around 2 (which is assumed to be identical for c and b quarks) to reproduce the data. Thus the difference from the data is of the order that we expect for the contribution from radiation energy loss, which is not included here.

In this article, we follow the labeling established in Ref. [3]. The approach with a running coupling constant is dubbed "model E." To emphasize the influence of the running coupling constant we present also some results for "model C," in which the coupling constant is taken as $\alpha_s(2\pi T)$ and $\mu^2 = 0.15 m_D^2$. This model requires K ≈ 5 to reproduce the RHIC data. In all calculations, presented here, the corresponding K factors have been applied.

D. Interaction of the heavy quark with the expanding plasma

The heavy quarks can scatter elastically with the gluons and light quarks that are present in the QGP. The temperature field, determined by the hydrodynamical calculations, allows us to calculate the density and—together with the local expansion velocity of the plasma—the momentum distribution of the light quarks and gluons that scatter with the heavy quark. The interaction is described by a Boltzmann equation, which is solved by the test particle method, applying Monte Carlo techniques. For the collisions between the heavy quarks and the plasma particles we apply the elementary pQCD cross sections. We follow the trajectory of the individual heavy quarks from creation until hadronization but do not pursue that of the plasma particles. Hadronization occurs when the energy density of the fluid cell falls under a critical value of the energy density. This is 1.64 GeV/fm^3 in the scenario without mixed phase and 0.5 GeV/fm^3 at the end of the mixed phase. It is assumed that after hadronization heavy mesons do not interact with the hadronic environment.

E. Hadronization

The heavy quarks form hadrons either by coalescence or by fragmentation. In our calculation the relative fraction depends on p_Q, on the fluid cell velocity, and on the orientation of the hadronization hypersurface Σ as explained in the following. The coalescence mechanism is based on the model of Dover [14]. To describe the creation of a heavy meson by coalescence we start from

$$N_{\Phi=D,B} = \int p_Q \cdot d\sigma_1 p_q \cdot d\sigma_2 \frac{d^3p_Q}{(2\pi\hbar)^3 E_Q} \frac{d^3p_q}{(2\pi\hbar)^3 E_q} \times f_Q(x_Q, p_Q) f_q(x_q, p_q) f_\Phi(x_Q, x_q; p_Q, p_q), \tag{4}$$

where f_Q and f_q are normalized to the number of quarks that go through the hypersurface:

$$\int p_Q \cdot d\sigma_1 \times f_Q(x_Q, p_Q) \frac{d^3p_Q}{(2\pi\hbar)^3 E_Q} = N_Q = 1 \tag{5}$$

for hadronization of a given heavy quark and

$$\int p_q \cdot d\sigma_2 \times f_q(x_q, p_q) \frac{d^3p_q}{(2\pi\hbar)^3 E_q} = N_q. \tag{6}$$

Here f_Φ is the invariant probability density that a heavy quark at the position x_Q with momentum p_Q forms a heavy meson Φ with a light quark with x_q, p_q, which traverses the hypersurface Σ. The function $f_q(x_q, p_q)$ is the distribution of the light quarks, which is assumed to be a thermal Boltzmann-Jüttner distribution. Assuming that f_Φ factorizes we use

$$f_\Phi(x_Q, x_q; p_Q, p_q) = \exp\left(\frac{(x_q - x_Q)^2 - [(x_q - x_Q)\cdot u_Q]^2}{2R_c^2}\right) F_\Phi(p_Q, p_q), \tag{7}$$

where u_Q is the four-velocity of the heavy quark. Thus in the rest system of the heavy quark f_Φ is a Gaussian function of $\|\vec{x}_q - \vec{x}_Q\|$. Coalescence requires that in coordinate space the positions of the heavy quark and of the light quark are very close and we obtain

$$N_\Phi = \int \frac{d^3p_q}{(2\pi\hbar)^3 E_q} \frac{p_q \cdot d\hat{\sigma}}{u_Q \cdot d\hat{\sigma}} f_q(x_Q, p_q)(\sqrt{2\pi}R_c)^3 \times F_\Phi(p_Q, p_q), \tag{8}$$

where $d\hat{\sigma}$ is the unit vector along $d\sigma$. The $u_Q \cdot d\hat{\sigma}$ denominator is positive if the heavy quark escapes from the plasma. It accounts for the fact that a heavy quark coming out tangentially to the critical hypersurface Σ has a larger chance of encountering its light partner. For $F_\Phi(p_Q, p_q)$ we take

$$F_\Phi(p_Q, p_q) = \exp\left(\frac{\left(\frac{p_Q}{m_Q} - \frac{p_q}{m_q}\right)^2}{2\alpha_d^2}\right). \tag{9}$$

The coalescence probability is maximal if $x_q = x_Q$ and $p_q = p_Q$. The normalization condition

$$\int \frac{d^3r d^3p}{(2\pi\hbar)^3} f_\Phi(x_Q, x_q, p_Q, p_q) = 1, \tag{10}$$

where r and p are the relative coordinates between Q and q, relates α_d^2 and R_c^2. We find

$$N_\Phi(x_Q; p_Q) = \frac{\tilde{c}_d g_q}{u_Q \cdot d\hat{\sigma}(x_Q)} \int_{u_q \cdot d\hat{\sigma}(x_Q)>0} \frac{d^3u_q}{u_0} u_q \cdot d\hat{\sigma}(x_Q) \times e^{-\left(\frac{m_q}{T_c} u_{\rm cell}(x_Q) + \frac{u_Q}{\alpha_d^2}\right)\cdot u_q}, \tag{11}$$

where g_q is the degeneracy factor of the light quarks, u_q is their four-velocity, and

$$\tilde{c}_d := \left(\frac{m_Q + m_q}{m_Q}\right)^3 \times \frac{1}{4\pi\alpha_d^2 K_2\left(\frac{1}{\alpha_d^2}\right)} \approx \frac{1}{4\pi\alpha_d^2 K_2\left(\frac{1}{\alpha_d^2}\right)} \tag{12}$$

if $m_Q \gg m_q$. For the calculation we assume a critical temperature of $T_c = 165$ MeV. Equation (11) is up to a factor the Cooper-Frye formula, which describes the hadronization of particles at the surface of the expanding plasma, with an effective inverse temperature $\beta_{\rm eff}$ and an effective four-velocity $u_{\rm cell,eff}$ such that $\beta_{\rm eff} u_{\rm cell,eff} = \beta_c u_{\rm cell} + \frac{u_Q}{\beta_c m_q \alpha_d^2}$. For a given choice of the mass m_q, we complete our coalescence algorithm by fixing α_d in such a way[2] that $N_B = 1$ for a b quark at rest in a fluid cell with $d\hat{\sigma} = u_{\rm cell}$, in agreement with the physical picture that such a heavy quark can hadronize exclusively by coalescence. The numbers N_D and N_B calibrated in this way are thus interpreted as coalescence *probabilities*, as illustrated in Fig. 2.

For momenta above $p_Q = 0.5$ GeV the probability to form a heavy meson by coalescence falls below one. Because all heavy quarks appear finally as heavy mesons we assume that all heavy quarks that do not coalesce form mesons by fragmentation, as described in Ref. [5]. As one can see in Fig. 2, high-p_T heavy mesons are formed exclusively by this mechanism.

[2]This leads to $\alpha_d = 0.88$ for $m_q = 100$ MeV and to $\alpha_d = 0.39$ for $m_q = 200$ MeV.

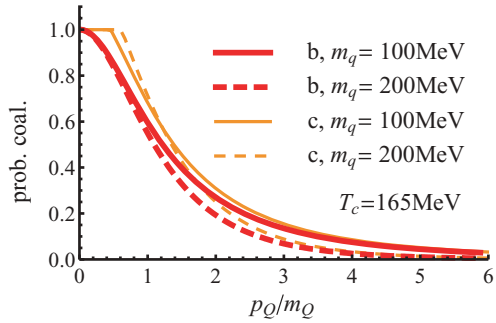

FIG. 2. (Color online) Relative contribution of coalescence of a c (b) quark with a light quark at freeze-out to the D (B) meson yield as a function of the relative momentum p_Q/m_Q of the heavy quark. Heavy mesons that are not produced by coalescence are created by fragmentation as described in Ref. [5].

By this hadronization procedure we get a good description of the p_T spectrum over the whole p_T range. The physics can best be discussed in terms of R_{AA}, which is expected to be one if no medium is present. Our results for the D and B mesons for central Au + Au collisions at RHIC are displayed in Fig. 3 (for the explication of the different models we refer to Ref. [3]). In this figure, the upper (lower) limit of the "D-meson" band for model E corresponds to $m_q = 100$ MeV ($m_q = 200$ MeV) in Eq. (11). For B mesons the difference between the two corresponding curves is of the order of the line width. In the following, we will retain $m_q = 100$ MeV.

III. TOMOGRAPHY AT RHIC ENERGIES

A. Momentum loss

We start our analysis with the investigation of the momentum loss the heavy quarks suffer while traversing the plasma. In Fig. 4 we display, for central Au + Au collisions at $\sqrt{s} = 200A$ GeV, the conditional probability density of the transverse momentum loss as a function of the initial momentum of the heavy quarks. At high initial momenta ($p_T > 5$ GeV) we observe a quite broad distribution, which

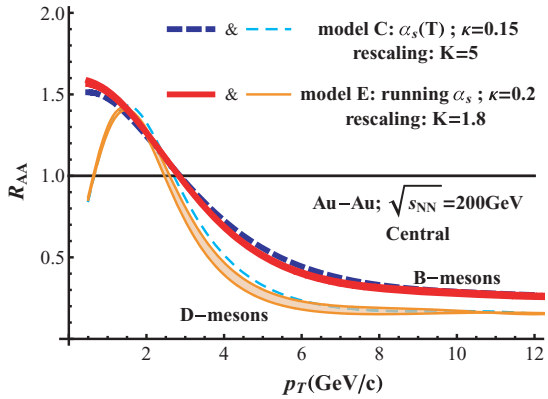

FIG. 3. (Color online) R_{AA} as a function of p_T for D and B mesons. We display R_{AA} for two parametrizations that describe the experimental data after the results have been multiplied with appropriate K factors (see Ref. [3] and Sec. II C for details).

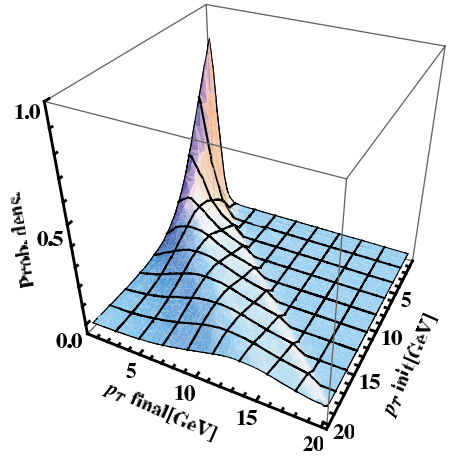

FIG. 4. (Color online) Mean value and variance of the final p_T momentum distribution of c quarks as a function of their momentum at production for central Au + Au collisions at $\sqrt{s} = 200$ GeV.

narrows for smaller p_T values. For very low initial momenta we see an increase of the transverse momentum during the expansion. If their initial p_T value is smaller than that expected for heavy quarks in equilibrium with their environment the interactions with the plasma particles increase their momenta. In Fig. 5 the mean value and the variance of this probability density are plotted. Above $p_T = 10$ GeV we observe, despite of the complex path-length distribution, to a very good approximation a linear dependence of the p_T loss on the initial p_T momentum, which can be described by $\langle p_T^{\text{final}} \rangle = p_T^{\text{initial}} - 0.08 p_T^{\text{initial}} - 5$ GeV. Numerically, the constant -5 GeV energy loss dominates the $-0.08 p_T^{\text{initial}}$ term even for high p_T^{initial} but for quantitative comparisons the latter is not negligible. This is consistent with the underlying microscopic energy loss, as $\frac{dE}{dx}$ was shown to saturate at large initial momenta because of asymptotic freedom [11]. Also, the variance depends linearly on the initial p_T value for high initial momenta. For low initial momenta the situation becomes more complex; there, the final p_T approaches the value expected for heavy quarks in equilibrium with their environment.

To allow for a comparison with other approaches, it is interesting to make the link between the energy loss of our model and the transport coefficient,

$$\hat{q} = \frac{\langle k_\perp^2 \rangle}{\lambda} = \langle k_\perp^2 \rangle \sigma \rho = \frac{1}{v_Q} \frac{\langle k_\perp^2 \rangle}{\Delta t} \approx \frac{4 B_\perp}{v_Q}, \tag{13}$$

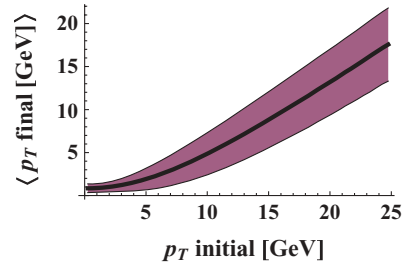

FIG. 5. (Color online) Mean value and variance of the conditional probability density for a c quark with a final transverse momentum p_T as a function of the initial p_T.

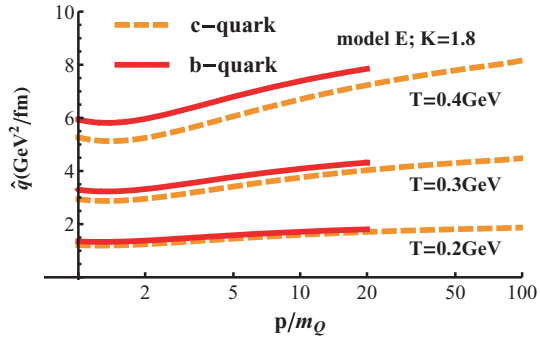

FIG. 6. (Color online) $\hat{q}$ as a function of the momentum of the heavy quark for the standard parameter set E and for three temperatures of the plasma [3].

which describes the average squared transverse momentum transfer in a single collision divided by the mean free λ. Here σ, ρ, $B_\perp$, Δt, and v_Q are the heavy quark parton cross section, the parton density in the medium, the transverse diffusion coefficient [3], the time between two subsequent collisions, and the heavy quark velocity, respectively. Figure 6 shows $\hat{q}$ as a function of the momentum of the heavy quark.

B. Dependence of the momentum loss on the creation point in coordinate space

The momentum loss of a heavy quark depends on the creation point of the heavy quark-antiquark pair. If one wants to know information about the QGP, which is contained in the measured p_T spectra, it is important to know from which part of the QGP the observed heavy quarks originate. Figure 7 shows, on the left-hand side, the average final p_T of the heavy (anti)quarks as a function of their initial p_T and of the transverse distance of their creation point with respect to the center of the reaction, $r_T^{\rm in}$. We see three different regimes. At low initial p_T the average final momentum is independent of the distance to the center. These are heavy quarks that come to an equilibrium with the environment. At large values of $r_T^{\rm in}$ the momentum loss is small because the heavy quarks are too close to the (in the hydrodynamical calculation shrinking) surface to interact with the plasma. The third type of heavy quarks are those that have initially a high momentum and have been created close to the center. These quarks are really penetrating probes traversing an important fraction of the plasma. The momentum loss of these particles is high but it does not change substantially in the range $0 < r_T^{\rm in} < 4$ fm. In other words, Fig. 7 shows an explicit path-length dependence, despite the rapid decrease of the energy density during plasma cooling. This fact contradicts the conclusion of Ref. [15]. A complementary view of the centrality dependence of the momentum loss is shown on the right-hand side of Fig. 7. There we plot the relative momentum loss as a function of the initial transverse momentum p_T and of the centrality. The relative momentum loss increases with centrality and with decreasing initial momentum. Heavy quarks with a moderate initial momentum suffer the heaviest relative momentum loss. There the kinematics of the collisions allows for large-angle scattering and therefore for a relatively fast approach to equilibrium. The kinematics of the collisions of fast heavy quarks with the thermal environment leads only to a moderate momentum transfer and therefore the direction of the heavy quark changes only little. Figure 8 (left) shows the dependence of $(dN/dp_T^{\rm fin(al)})/(dN/dp_T^{\rm in(itial)})$ on the production point of the charmed quark-antiquark pair. Pairs produced at the center of the reaction are highly suppressed at large p_T. Therefore quarks that contribute in this kinematical regime are predominantly from the surface and contain little information on plasma properties in the center of the reaction. This corona effect can be illustrated alternatively by using the correlation between the average initial transverse position

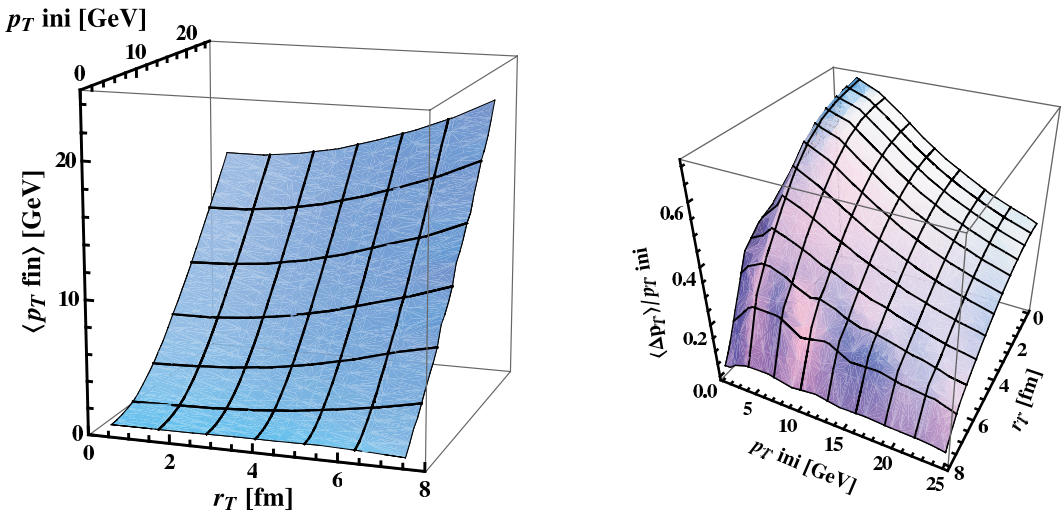

FIG. 7. (Color online) (Left) Average final momentum of the c quark as a function of its initial momentum and of the centrality of its creation point. (Right) Relative momentum loss of the heavy quark as a function of its initial momentum and of the centrality of its creation point. All calculations are done for central Au + Au collisions at $\sqrt{s} = 200$ GeV.

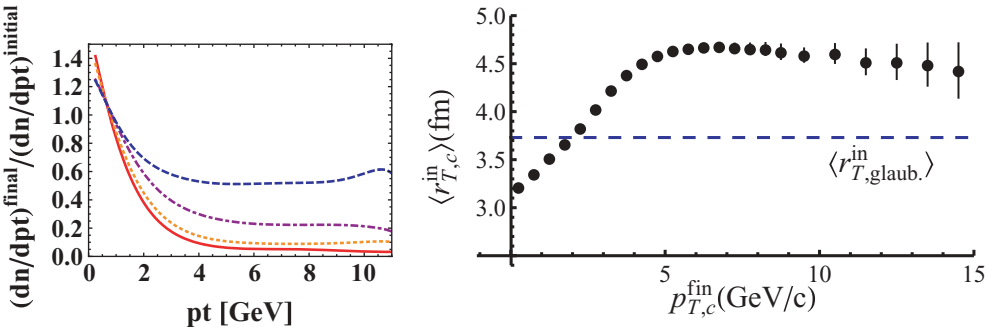

FIG. 8. (Color online) (Left) $(dN/dp_T^{\mathrm{fin(al)}})/(dN/dp_T^{\mathrm{in(itial)}})$ of c quarks produced at transverse distances of 0–2 fm (full), 2–4 fm (short-dashed), 4–6 fm (dashed-dotted), and 6–8 fm (dashed) to the "center" (symmetry axis) of the reaction for central Au + Au collisions at $\sqrt{s} = 200$ GeV. (Right) Average transverse position of the production points of the c quarks as a function of their final momentum. The dashed line corresponds to the p_T averaged position. The bars mark the statistical uncertainties in the simulations.

and the final transverse momentum[3] displayed in Fig. 8 (right). There one can see that heavy quarks, passing the hadronization hypersurface with $p_T \leqslant 3$ GeV, originate from larger initial transverse distances than the overall Glauber average ($\approx$3.7 fm). Heavy quarks with a small final transverse momentum come from production points that are more central than the average. We observe a (slow) decrease of $\langle r_T^{\mathrm{in}} \rangle$ for large values of p_T, because with increasing $p_{T,c}^{\mathrm{fin}}$ the matter becomes less and less opaque (see Fig. 7).

We now discuss a possible way to use the $Q\bar{Q}$ pair as a trigger to probe inner regions of the QGP. Within our model, each $Q\bar{Q}$ pair is initially created back to back with the same momentum.[4] For the most central production points, the final momentum difference is small because the path lengths in the plasma are almost the same for both quarks. The more peripheral the pair is produced the more the effective path lengths in the QGP can be different. Therefore, the smaller the final p_T difference of the simultaneously produced c and $\bar{c}$ pair the more it is probable that it has been produced at a small distance from the center. Our approach thus predicts a strong correlation between the final transverse-momentum difference of a given $Q\bar{Q}$ quark pair and its initial position in the transverse plane. This correlation could possibly be exploited experimentally to discriminate this model from other approaches where energy loss is not due to multiple independent collisions. In Fig. 9 (left), we study further this correlation for simultaneously created $c\bar{c}$ pairs. We display the average transverse distance $\langle r_T^{\mathrm{in}} \rangle$ of their production points to

[3]Whereas in dynamical evolution, it is the initial position that (partly) determines the heavy-quark evolution and its final momentum before hadronization, it is quite natural, in this type of "reverse analysis," to perform selections on final observables and to investigate how they permit us to access former properties of the distribution.

[4]Next-to-leading-order corrections spoil of course this idealized view; they are expected to be large at LHC for $c\bar{c}$ pairs.

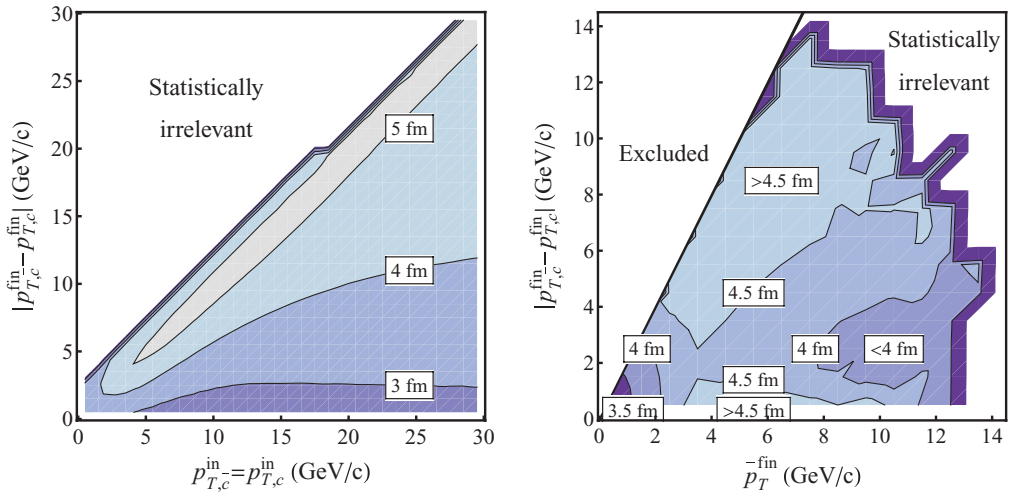

FIG. 9. (Color online) (Left) Correlation between the average centrality $\langle r_T^{\mathrm{in}} \rangle$ of the production points of the $c\bar{c}$ pair (labeled isocontours, in femtometers) and the difference between the final momenta of the quarks, $\Delta p_T^{\mathrm{fin}} := |p_{T,c}^{\mathrm{fin}} - p_{T,\bar{c}}^{\mathrm{fin}}|$, for various initial momenta $p_{T,c}^{\mathrm{in}} = p_{T,\bar{c}}^{\mathrm{in}}$. (Right) The same correlation as left but for various final pair momenta $\bar{p}_T^{\mathrm{fin}} := \frac{p_{T,c}^{\mathrm{fin}} + p_{T,\bar{c}}^{\mathrm{fin}}}{2}$.

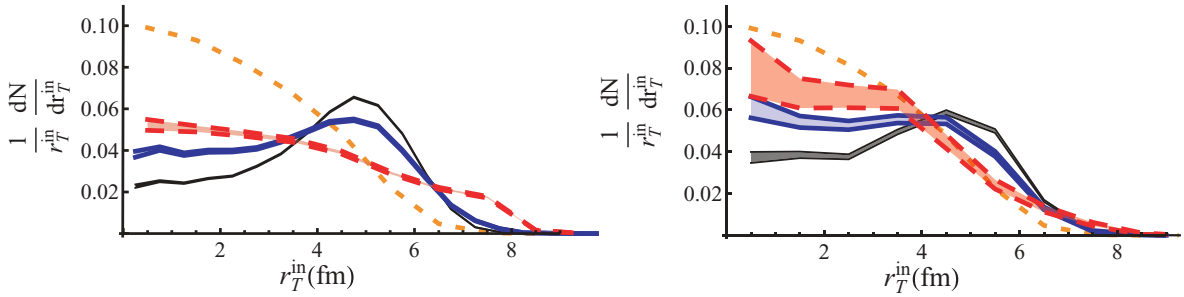

FIG. 10. (Color online) (Left) Distribution of the radial distance $r_T^{\rm in}$ of the production points of the $c\bar{c}$ pairs for various conditions on their final momenta: no selection (dotted, orange), $p_{T,c}^{\rm fin} > 5$ GeV (thin, black), $\bar{p}_T^{\rm fin} > 5$ GeV (thick, blue), and $\bar{p}_{T,c}^{\rm fin} > 5$ GeV $\cap\ \Delta p_T^{\rm fin} < 0.2\,\bar{p}_T^{\rm fin}$ (dashed, red). All distributions are normalized to unity. (Right) The same distributions, but with a lower bound of p_T of 10 GeV instead of 5 GeV.

the center of the reaction as a function of the initial (anti)quark momentum $p_T^{\rm in}$, separated for different values of the final momentum difference between the c and the $\bar{c}$ quark. For $p_T^{\rm in} > 5$ GeV, one sees the expected correlation: The quarks of pairs created far from the center ($\langle r_T^{\rm in}\rangle$ large) usually have quite different path lengths and show therefore finally a large momentum difference $\Delta p_T^{\rm fin}$. In contrast, for quarks created close to the center the path length is similar and therefore $\Delta p_T^{\rm fin}$ is small. Therefore, by selecting events with small $\Delta p_T^{\rm fin}$ (with respect to $p_T^{\rm in}$), one can trigger on more central events to study their properties.

In practice, one does of course not have access to $p_T^{\rm in}$ as we only measure particles in their asymptotic state. Therefore it is useful to study the same correlation as a function of the average between $p_{T,c}^{\rm fin}$ and $p_{T,\bar{c}}^{\rm fin}$ (i.e., $\bar{p}_T^{\rm fin} := \frac{p_{T,c}^{\rm fin}+p_{T,\bar{c}}^{\rm fin}}{2}$). This is done in Fig. 9 (right). Owing to the energy loss the structure has changed as compared to the left panel. We find now that for intermediate values of $\bar{p}_T^{\rm fin}$ ($\in [3, 10]$ GeV), requesting $\Delta p_T^{\rm fin} \approx 0$ leads to *larger* values of $\langle r_T^{\rm in}\rangle$, of the order of 5 fm. A refined analysis shows that this small-$\Delta p_T^{\rm fin}$ crest is due to pairs that are produced peripherally and tangentially to the fireball cylinder ($\vec{p}_T^{\rm in} \perp \vec{x}_T^{\rm in}$). Hence the trajectories of both quarks have approximately the same path length in matter. Although these events are much less frequent than $c\bar{c}$ production inside the bulk of the QGP, the associated energy loss is rather small, and $p_{T,c}^{\rm fin} \approx p_{T,c}^{\rm in}$, so that they dominate the final spectra because of the steeply falling $\frac{d\sigma_{\rm prod}}{dp_T^{\rm in}}$. This interpretation is confirmed by analyzing the radial distribution of the creation points, $r_T^{\rm in}$, for different conditions on $\bar{p}_{T,c}^{\rm fin}$, as shown in Fig. 10 (left). For large final p_T values, $p_{T,c}^{\rm fin} > 5$ GeV or $\bar{p}_T^{\rm fin} > 5$ GeV, the corona effect is manifest and the central $r_T^{\rm in}$ region is clearly depleted with respect to the minimum-bias Glauber distribution (short dashed line). Imposing an additional cut on $\Delta p_T^{\rm fin}$, $\Delta p_T^{\rm fin} < 0.2\,\bar{p}_T^{\rm fin}$, we observe the disappearance of the corona peak together with a moderate enrichment of the central $r_T^{\rm in}$ values and an extended "hyper corona" shoulder located at $r_T^{\rm in} \approx 6$–8 fm, where those tangential emissions take place, in which both quarks lose very little energy and therefore $\Delta p_T^{\rm fin} \approx 0$. The right-hand side of Fig. 9 shows how one can trigger on more central collisions. Increasing values of $\bar{p}_T^{\rm fin}$ increase the sensitivity to central events. With the condition $\bar{p}_T^{\rm fin} > 10$ GeV, $\Delta p_T^{\rm fin} \in [1\text{ GeV}, 4\text{ GeV}]$, the sample of events is close to that expected from the Glauber distribution. The reason for this is that in pQCD calculations with increasing energy of the heavy quarks the plasma becomes more transparent, as seen on Fig. 7 (right). Energetic heavy quarks produced at small r_T are hence more likely to leave the plasma with an appreciable energy and thus they compete in number with quarks produced peripherally. Therefore, in the right panel of Fig. 9 $\langle r_T\rangle$ decreases for large $\bar{p}_T^{\rm fin}$. From Fig. 10 (right) we see that we nearly recover the Glauber distribution when we apply simultaneously a $\Delta p_T^{\rm fin} < 0.2\bar{p}_T^{\rm fin}$

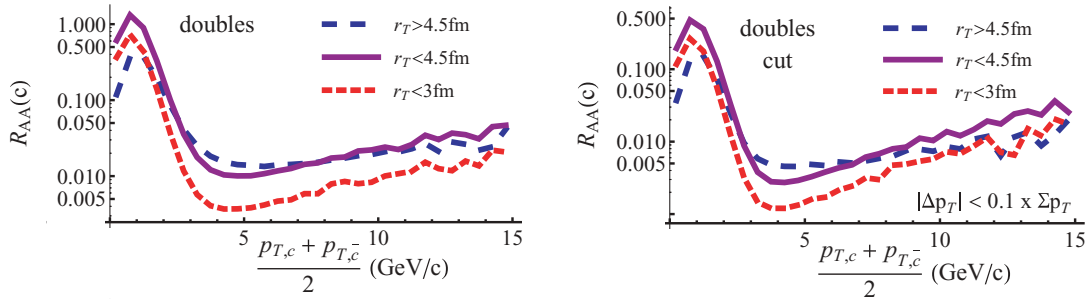

FIG. 11. (Color online) $R_{AA}(\bar{p}_T)$—here defined has the ratio $(dN/d\bar{p}_T^{\rm fin})/(dN/d\bar{p}_T^{\rm in})$ as a function of the average of the momenta of the simultaneously produced pair—for different conditions of the transverse momentum difference $\Delta p_T^{\rm fin}$ between the c and the $\bar{c}$ quark and various selections on the transverse distance $r_T^{\rm in}$ of the pair creation points with respect to the center of the reaction. The left panel shows R_{AA} for all possible $\Delta p_T^{\rm fin}$ and three different bins of $r_T^{\rm in}$; the right panel shows the result if we apply in addition a cut on the relative transverse momentum of the pair.

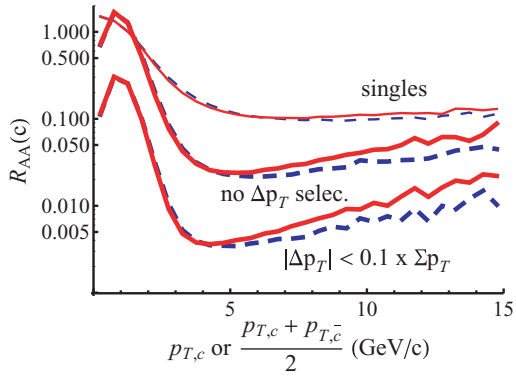

FIG. 12. (Color online) R_{AA} of c quarks. The thin line refers to single quarks; thick lines correspond to the R_{AA} of $\bar{p}_T$ with and without a $\Delta p_T^{\rm fin}$ selection (as in Fig. 11). The full (dashed) line refers to model E (C) [3].

and a $\bar{p}_T^{\rm fin} > 10$ GeV cut. Another consequence of this increasing transparency is seen in Figs. 11 and 12. There, we display $R_{AA}(\bar{p}_T) = (dN/d\bar{p}_T^{\rm fin})/(dN/d\bar{p}_T^{\rm in})$ of $c\bar{c}$ pairs for different $\Delta p_T^{\rm fin}$ selections in comparison with the $R_{AA}(p_{T,c/\bar{c}})$ of single (anti)charm quarks (Fig. 12). Only at small p_T does $dN/dp_T^{\rm in}$ differ from $dN/d\bar{p}_T^{pp}$ owing to the Cronin effect, discussed in Sec. II B. Therefore for larger p_T $R_{AA}(\bar{p}_T)$ is a quantity that can be measured. All curves in Fig. 11 show a minimum around $p_T \approx 5$ GeV where the relative energy loss is most important. The increase beyond $p_T \approx 5$ GeV becomes larger if we consider the production versus $\bar{p}_T$ and even larger if we limit the relative transverse momentum of the pair. Although the second observation is clearly expected, the first one, that R_{AA} behaves differently as a function of $\frac{p_{T,c}+p_{T,\bar{c}}}{2}$ than as a function of $p_{T,c}$ is astonishing and demands some explanation in view of the similar $\frac{dN}{dr_T}$ profiles observed in Fig. 10. A detailed analysis shows that the fluctuations of the *average* $\frac{p_{T,c}+p_{T,\bar{c}}}{2}$ are smaller than that of the momentum of each of the quarks only. Therefore, the energy loss is less washed out and this explains the p_T dependence of R_{AA}.

In conclusion, several relations can be used to validate pQCD-based models in general as well as our particular model if coincidence data become available because the dependence of R_{AA} as a function of $\bar{p}_T$ for different $\Delta p_T^{\rm fin}$ reflects directly the interaction of the quarks with the expanding plasma, especially the energy loss as a function of p_T. For calculations with a running coupling constant (E) the increasing transparency for large-p_T quarks is more pronounced than for those with a fixed coupling constant (C). A Δp_T cut can be used to achieve a robust characterization of the energy-loss mechanism of heavy quarks. The heavy-quark pairs are therefore one of the few probes that are sensitive to the expansion of the plasma and not only to its properties at the chiral/confinement phase transition. Although we have concentrated our analysis on the heavy *quarks* and not on the observed heavy mesons, we expect that the physics seen in Fig. 12 does not change because of hadronization. Next-to-leading-order effects at the level of $Q\bar{Q}$ production may modify slightly the conclusions and should be included in future work.

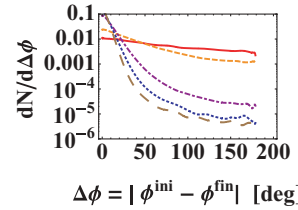

FIG. 13. (Color online) Distribution of $\Delta\phi$ for different initial p_T bins: 0–2 GeV (full), 2–5 GeV (dashed), 5–10 GeV (dashed-dotted), 10–15 GeV (dotted), and >15 GeV (long dashed).

We see a very complex behavior of the momentum loss of heavy quarks in an expanding QGP. It is therefore more than questionable that quantitative predictions of the energy loss are possible in models that are based on the average path length of the heavy-quark trajectory in the plasma.

C. Azimuthal correlations between simultaneously produced c and $\bar{c}$

Because of the large mass of the heavy quark, interactions between a heavy quark and a plasma particle change the direction of the heavy quark only little. We therefore expect that the final azimuthal angle is strongly correlated with the initial one. This is indeed the case for sufficiently high p_T values, as seen in Fig. 13. There we display the distribution of the difference between initial and final azimuthal angle of heavy quarks for different initial p_T intervals. The higher p_T the more small-angle scattering dominates and the more we see a correlation between initial and final azimuthal angle. There is a sharp transition toward an almost flat distribution for $p_T^{\rm initial} < 5$ GeV. As already seen, the kinematics allows quarks with this initial p_T to come (almost) to an equilibrium with the environment and therefore the correlation is weakened.

IV. COMPARISON WITH AdS/CFT AT RHIC

A completely different approach to explain the energy loss of heavy mesons and hence of the observed low R_{AA} value at high p_T has recently been launched by Horowitz and Gyulassy [16]. Their model is based on the assumption that QCD is similar to supersymmetric Yang-Mills theory and that this theory is dual to string theory in the limit of large $N_{\rm color}$. Whether this assumption is justified or not has to be verified. The model allows them to calculate the momentum loss

$$\frac{dp_T}{dt} = -\text{const}\frac{T^2}{M_q}\, p_T. \tag{14}$$

After having implemented this energy loss in a Fokker-Planck approach [17] they could predict quite a number of observables, which can be confronted with pQCD predictions. One of the observables for which the predictions are quite different is the relative energy loss of c and b quarks.

Perturbative QCD calculations show a much weaker mass dependence (for a given p_T). Besides a mass dependence of the energy loss in the subdominant u channel of the $gQ \to gQ$, which is $\propto \frac{T^2}{m_Q^2}$, the energy loss is only mass dependent for

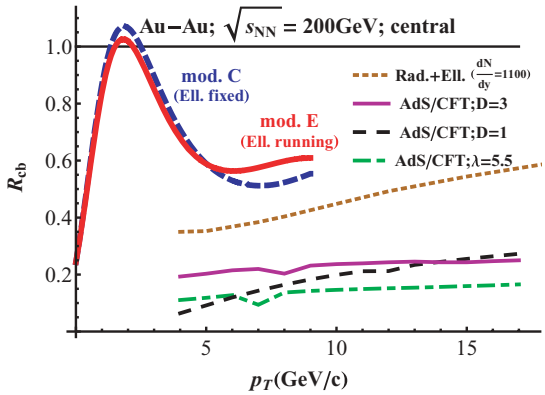

FIG. 14. (Color online) $R_{cb}(p_T) = R^c_{AA}(p_T)/R^b_{AA}(p_T)$ for different theories. We compare the pQCD-based "collisional" models C (with K = 5, blue) and E (with K = 1.8, red) [3] with the AdS/CFT calculation for different drag coefficients $D/2\pi T$ [16] and for $\lambda = 5.5$ [16,18] as well as with a pQCD calculation with a fixed coupling constant including radiative collisions [17].

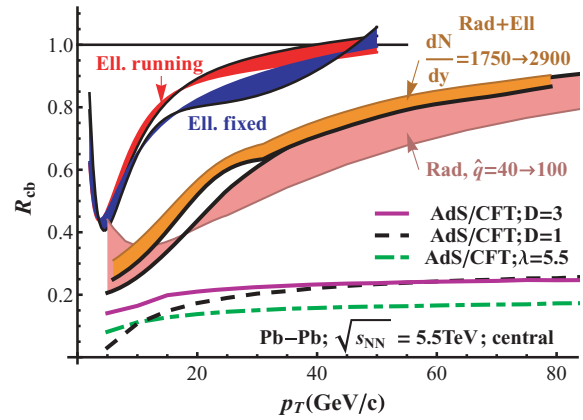

FIG. 16. (Color online) $R_{cb}(p_T) = R^c_{AA}(p_T)/R^b_{AA}(p_T)$ for different theories and for central Pb + Pb collisions at 5.5 *A* TeV. We compare the pQCD-based models C (with K = 5, blue) and E (with K = 1.8, red) [3] with the AdS/CFT calculation for different drag coefficients $D/2\pi T$ [16] and for $\lambda = 5.5$ [16,18] and with the pQCD calculation with constant coupling, which includes as well radiative energy loss [17].

intermediate p_T ($m_Q \ll p_T \ll \frac{m_Q^2}{T}$), where $\frac{dE}{dx} \propto \ln(\frac{p_Q}{m_Q})$ in the case of fixed α_s. Therefore the difference between the two theories can be made evident by comparing the $R_{AA}(p_T)$ for bottom and charm quarks. For this purpose one may define $R_{cb}(p_T) = R^c_{AA}(p_T)/R^b_{AA}(p_T)$ [17]. In Fig. 14 we compare the results of the different theories. It is evident that already the experiments at RHIC energies allow us to discard one of the theories if high-p_T D and B mesons could be identified.

Our model yields quite large values of R_{cb} because of the small value of the IR regulator. Perturbative QCD calculations with a fixed coupling constant [17] yield smaller values. Owing to the mild dependence on m_Q, mentioned before, $R^c_{AA}(p_T^{\rm fin}) \approx R^b_{AA}(p_T^{\rm fin})$ as soon as the initial momentum distributions become similar, $\frac{dN_c}{dp_T} \approx \frac{dN_b}{dp_T}$. This is the case for $p_T^{in} \geqslant$ 20 GeV/*c* (see Fig. 1).

V. PREDICTIONS FOR LHC

Going from the known RHIC to the unknown LHC energy domain we are faced with the problem of not knowing how the properties of the QGP change with increasing energy.

We therefore give our results for a range of charged particle multiplicities, $1600 < dN_{\rm ch}/dy(y = 0) < 2200$, that have been predicted for LHC. We assume furthermore that the eccentricity in coordinate space remains the same. Figure 15 shows the expected R_{AA} as a function of p_T for D and B mesons for model E of Ref. [3], which describes best the experimental data at RHIC. This model has a K factor of 1.8. We see that at LHC we will experimentally cover the p_T region in which R_{AA} increases with p_T. Nevertheless, the R_{AA} values are still far away from 1, as expected for $p_T \to \infty$.

The larger p_T range at LHC will make it possible to discriminate unambiguously between the different energy-loss models. Figure 16 shows $R_{cb}(p_T)$ for three different theories: AdS/CFT [16], pQCD with radiative energy loss and constant coupling constant [17], and our collisional energy-loss model with a K factor of 1.8 (5) for running (fixed) α_s. For moderate p_T ($p_T < 20$ GeV) the spectral form of the *c* and *b* quarks is different and $R_{cb}(p_T)$ is far from 1, despite the fact that the energy loss becomes more and more similar for *c* and

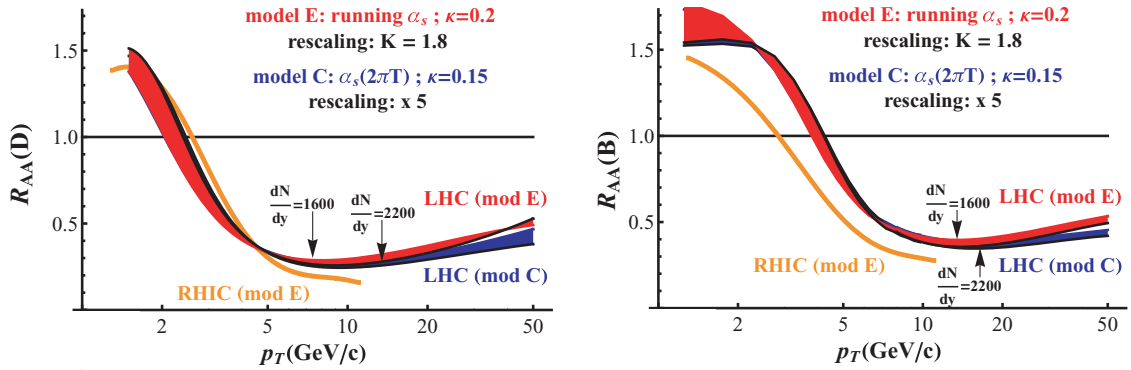

FIG. 15. (Color online) R_{AA} for central Pb + Pb collisions at 5.5 *A* TeV as a function of p_T for D (left) and B (right) mesons for model E of Ref. [3] for LHC energies as compared to RHIC energies.

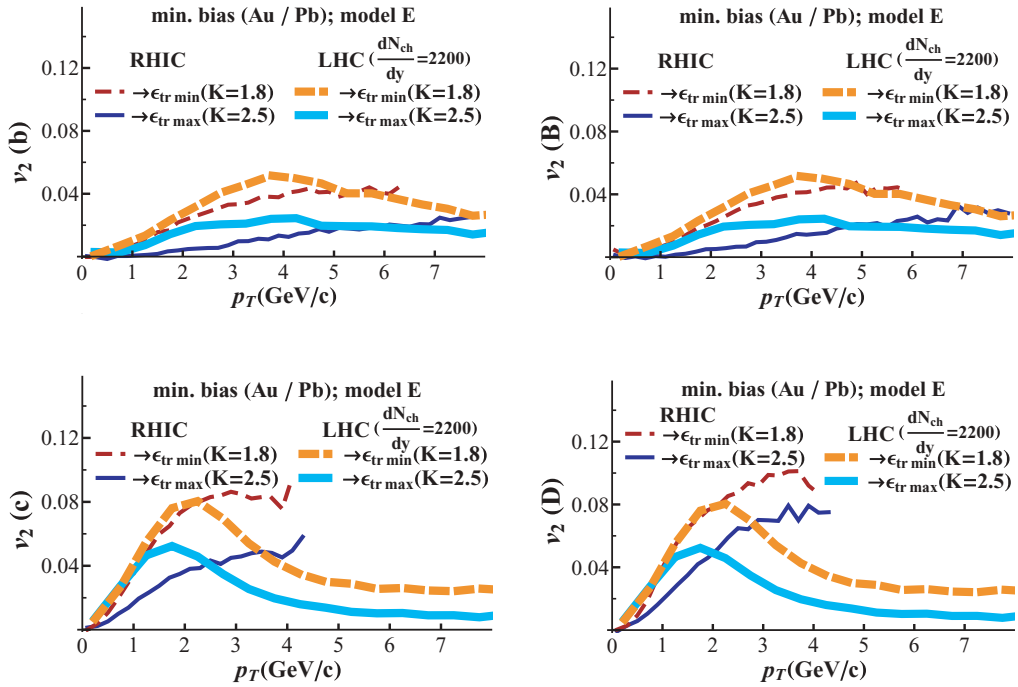

FIG. 17. (Color online) v_2 for minimum-bias reactions Au + Au at 200 A GeV and Pb + Pb at 5.5 A TeV for model E [3]. The K factors are noted in the text. The top row shows b quarks (left) and B mesons (right); the bottom row shows c quarks (left) and D mesons (right).

b quarks. Above $p_T = 30$ GeV an identical spectral form of the quarks and a constant energy loss results in $R_{cb}(p_T) \approx 1$. Perturbative QCD calculations are bound to arrive finally at values of $R_{cb}(p_T)$ close to one owing to the weak mass dependence of the cross section. The detailed form of R_{cb} depends on the cross sections or, more explicitly, on the form of the coupling constant and of the IR regulator employed in the pQCD cross-section calculation. In contrast, AdS/CFT predicts even for the highest momenta $R^{cb} = 0.2$–0.3, but it has not been demonstrated yet up to which p_T values the approximations of the approach remain valid.

The azimuthal anisotropy, which has been observed at RHIC energies, will remain visible up to LHC energies, as can be inferred from Fig. 17, where we display v_2 for minimum-bias events separated for b quarks (top left), B mesons (top right), c quarks (bottom left), and D mesons (bottom right). Here "$\epsilon_{\text{tr min}}$" means hadronization at the end of the mixed phase and "$\epsilon_{\text{tr max}}$" means hadronization at the end of the pure QGP phase; in the latter case, a K factor of K = 2–3 has to be applied to reproduce the experimental R_{AA} values for the most central events. In Ref. [3] we found that the experimental values at RHIC can only be reproduced when the hadronization takes place at the *end* of the mixed phase. As is the case for the light hadrons at RHIC, also the v_2 of heavy mesons follows a hydrodynamical behavior until $p_T \approx 2$ GeV but the absolute value of v_2 is only about half of that of light hadrons.

VI. CONCLUSION

We have described in detail the predictions of the approach that we have advanced recently to describe the energy loss and the azimuthal anisotropy of heavy quarks in the environment produced in heavy-ion collisions and have extended our calculation toward LHC energies. It is based on pQCD calculations with a running coupling constant and an IR regulator derived from hard thermal loop calculations. As shown in Ref. [3], with these new ingredients the energy loss from elastic collisions is (up to a factor of about 2) sufficient to produce the observed $R_A A$ at RHIC collisions. We have presented several observables that allow us to test this model. In particular, we predict a large azimuthal anisotropy, even at LHC energies and strong correlations between R_{AA} and the transverse-momentum difference between the simultaneously produced $Q\bar{Q}$ pair. Correlations between simultaneously produced heavy quark pairs will allow for triggering on central collisions. The identification of D and B mesons will reveal whether AdS/CFT describes the passage of heavy quarks through matter or whether we are still in the realm of pQCD.

ACKNOWLEDGMENTS

We thank W. Horowitz for communicating his results and R. Vogt for communicating the p_T distribution of c and b quarks in pp collisions for LHC energies as well as for her fruitful comments on a preliminary version of this article.

[1] B. I. Abelev *et al.* (STAR Collaboration), Phys. Rev. Lett. **98**, 192301 (2007).

[2] A. Adare *et al.* (PHENIX Collaboration), Phys. Rev. Lett. **98**, 172301 (2007).

[3] P. B. Gossiaux and J. Aichelin, Phys. Rev. C **78**, 014904 (2008).
[4] M. Cacciari and P. Nason, Phys. Rev. Lett. **89**, 122003 (2002); M. Cacciari, S. Frixione, M. L. Mangano, P. Nason, and G. Ridolfi, J. High Energy Phys. 07 (2004) 033; M. Cacciari and P. Nason, *ibid.* 09 (2003) 006.
[5] M. Cacciari, P. Nason, and R. Vogt, Phys. Rev. Lett. **95**, 122001 (2005).
[6] R. Vogt (private communication).
[7] J.-C. Peng and M. Leitch (private communication).
[8] P. Kolb and U. Heinz, in *Quark Gluon Plasma 3*, edited by R. Hwa and X. N. Wang (World Scientific, Singapore, 2004), p. 634.
[9] B. Svetitsky, Phys. Rev. D **37**, 2484 (1988).
[10] B. L. Combridge, Nucl. Phys. **B151**, 429 (1979).
[11] A. Peshier, arXiv:hep-ph/0601119; Phys. Rev. Lett. **97**, 212301 (2006).
[12] E. Braaten and R. D. Pisarski, Phys. Rev. D **45**, R1827 (1992).
[13] E. Braaten and M. H. Thoma, Phys. Rev. D **44**, 1298 (1991); **44**, R2625 (1991).
[14] C. B. Dover, U. W. Heinz, E. Schnedermann, and J. Zimanyi, Phys. Rev. C **44**, 1636 (1991).
[15] H. Z. Huang, talk given at the workshop "Characterization of the Quark Gluon Plasma with Heavy Quarks," Bad Honnef, Germany, 26–28 June 2008, http://heavy-quarks.physi.uni-heidelberg.de/Agenda/Talks/H._Huang.ppt.
[16] W. A. Horowitz and M. Gyulassy, talk presented at the 20th International Conference on Ultra-Relativistic Nucleus-Nucleus Collisions: Quark Matter 2008 (QM2008), Jaipur, India, 4–10 Feb. 2008, arXiv:0804.4330 [hep-ph].
[17] S. Wicks, W. Horowitz, M. Djordjevic, and M. Gyulassy, Nucl. Phys. **A783**, 493 (2007); S. Wicks and M. Gyulassy, J. Phys. G **34**, S989 (2007).
[18] S. S. Gubser, Phys. Rev. D **76**, 126003 (2007).